microbial biotechnology

An innovative protein expression system using RNA polymerase I for large-scale screening of high-nucleic-acid content *Saccharomyces cerevisiae* strains

Duwen Zeng,[1] Chenxi Qiu,[2] Yu Shen,[2] Jin Hou,[2] Zailu Li,[1] Jixiang Zhang,[3] Shuai Liu,[3] Jianli Shang,[3] Wensheng Qin,[4] Lili Xu[1,2,3]* (iD) and Xiaoming Bao[1,2]

[1]*College of Bioengineering, Key Laboratory of Shandong Microbial Engineering, State Key Laboratory of Biobased Material and Green Papermaking, Qilu University of Technology, Shandong Academy of Sciences, 3501 Daxue Road, Jinan, 250353, China.*

[2]*State Key Laboratory of Microbial Technology, Institute of Microbial Technology, Shandong University, 72 Binhai Road, Qingdao, 266237, China.*

[3]*Shandong Sunkeen Biological Company, 6789 Xingfuhe Road, Jining, 273517, China.*

[4]*Department of Biology, Lakehead University, 955 Oliver Road, Thunder Bay, ON P7B 5E1, Canada.*

Summary

Saccharomyces cerevisiae **is the preferred source of RNA derivatives, which are widely used as supplements for foods and pharmaceuticals. As the most abundant RNAs, the ribosomal RNAs (rRNAs) transcribed by RNA polymerase I (Pol I) have no 5′ caps, thus cannot be translated to proteins. To screen high-nucleic-acid content yeasts more efficiently, a cap-independent protein expression system mediated by Pol I has been designed and established to monitor the regulatory changes of rRNA synthesis by observing the variation in the reporter genes expression. The elements including Pol I-recognized** *rDNA* **promoter, the internal ribosome entry site from cricket paralytic virus which can recruit ribosomes internally, reporter genes (***URA3*** and** *yEGFP3***),** *oligo-dT* **and an** *rDNA* **terminator were ligated to a yeast episomal plasmid. This system based on the** *URA3* **gene worked well by observing the growth phenotype and did not require the disruption of cap-dependent initiation factors. The fluorescence intensity of strains expressing the** *yEGFP3* **gene increased and drifted after mutagenesis. Combined with flow cytometry, cells with higher GFP level were sorted out. A strain showed 58% improvement in RNA content and exhibited no sequence alteration in the whole expression cassette introduced. This study provides a novel strategy for breeding high-nucleic-acid content yeasts.**

Introduction

Saccharomyces cerevisiae is a Generally Regarded As Safe (GRAS) microorganism and the preferred industrial source of RNA (Nagodawithana, 1992). RNA degradation products and their derivatives have many beneficial uses, especially in food and medical industry, and have important implications for improving the overall economic productivity of the yeast industry. For example, 5′-inosine monophosphate (5′-IMP) and 5′-guanine monophosphate (5′-GMP) can be safely used as food additives (Olmedo *et al.*, 1994; Zhao and Fleet, 2005; Cairoli *et al.*, 2008), while the derivatives of ribonucleotides (e.g. pyrimidines and purines) can be used as raw materials for food and pharmaceutical intermediates and so on (Rudolph *et al.*, 1990).

About 80% of total RNAs in yeast cells are ribosomal RNAs (rRNAs) (Warner, 1999), therefore, an effective way to increase RNA content is to enhance rRNA biosynthesis. The transcription of rRNAs (the primary transcript is 35S pre-rRNA) is efficiently and tightly regulated by RNA polymerase I (Pol I) and other factors through the ribosomal DNA promoter (*rDNAp*) (Planta, 1997; Hannan *et al.*, 1998). The *rDNA* genes are located on chromosome XII and consist of 150 to 200 repeated copies of a 9.1-kb unit in *S. cerevisiae* (Petes, 1979). For breeding higher RNA content strains, the screening model of the poor growth mutagenized cells on higher concentration (1.5 mol l^{-1}) KCl was used in *Candida* yeast in the early patent (U.S. Pat. No. 3,909,352,

Akiyama *et al.*, 1975). However, the mechanism of such screening model and the association between KCl and rRNA synthesis was not mentioned. Rational disruption of some functional genes can change rRNA synthesis and was thus used to set up the screening models. In Prof. Harashima's study, the non-essential gene *RRN10*, encoding a subunit of the upstream activation factor for rRNA transcription initiation, was disrupted in diploid cells. The tiny colonies grown from single cell by the tet-rad analysis from asci were picked up as the parental strain with poor growth phenotype. After mutagenesis, one of the growth-recovering suppressors showed RNA content twofold and 1.3-fold higher than the *Δrrn10* and the parental strain, respectively. The reason could be the detected upregulation of the *RPL40A* and *RPL40B* genes, which encode the components of the 60S large ribosomal subunit. When the *RRN10* was integrated into the suppressor genome, the total RNA content became twofold higher than in the parental strain (Chuwattanakul *et al.*, 2011; Khatun *et al.*, 2013). Actually, *RRN10* is an important gene for promoting a high level of transcription of *rDNA*, but based on its deletion (*Δrrn10*), cells with higher RNA content were still screened out (Chuwattanakul *et al.*, 2011), indicating that to explore more efficient elements for enhancing RNA content and to understand rRNA synthesis mechanism is still challenging. On the other hand, such depending on cell poor growth screening model seems difficult to pick up the tiny colonies, since the better growth cells normally gave strong background on the plates. Meanwhile, in *Candida tropicalis*, the two heterologous genes were introduced for perturbing the redox force. The RNA content was increased 5.5% by the membrane-bound transhydrogenase gene *pntAB* but decreased 10.6% by the NADH oxidase gene *noxE* (Li *et al.*, 2019). Fermentation parameters can also affect RNA yield to some extent: for example, pH 4.0 favoured the RNA accumulation in *Candida* yeast (Li *et al.*, 2012).

This handful of research data showed that there are still limitations in both breeding of high RNA content yeasts and screening out such yeast cells in large scale. The screening model based on the Pol I-mediated expression system might be powerful for these purposes, since the major components rRNAs were synthesized by Pol I. Generally, observing the variation in a reporter gene expression is one of the effective strategies to detect changes in regulatory mechanism. Unlike Pol II, which transcribes and processes mRNA by adding a 5′ cap and a 3′ poly-A tail, Pol I cannot mediate such post-transcriptional modifications (Sims *et al.*, 2004; Buratowski, 2009; Heidemann *et al.*, 2013), the resulting rRNAs cannot be translated to proteins, even they play roles in the process of translation. This provides great challenges for establishment of a Pol I-mediated protein expression system, as well as observing changes in regulation of rRNA synthesis.

In eukaryotes, the mRNA 5′ cap (^{m7}GpppN) is normally necessary for the initial stage of protein synthesis. It is recognized by a series of translation initiation factors (eIFs) together with Met-tRNA$_i^{Met}$ to recruit 40S small ribosomal subunits and form a preinitiation complex (Aitken and Lorsch, 2012). This is called a 5′ cap-dependent translation initiation process. On the other hand, the internal ribosome entry sites (IRESs) can mediate cap-independent translation initiation, since their secondary structure can recruit ribosomes internally (Pfingsten *et al.*, 2006). IRESs were discovered in picornavirus first (Pelletier and Sonenberg, 1988), then in other eukaryotic viruses (Reynolds *et al.*, 1995; Ohlmann, 2000). IRESs were also found in some mRNAs of cellular organisms and functioned when cells are under special stress conditions, such as heat shock, hypoxia, nutrient deprivation and so on (Holcik *et al.*, 1999; Holcik and Sonenberg, 2005; Gilbert *et al.*, 2007; Reineke *et al.*, 2011). The specific conserved IRES sequence in genome of hepatitis C virus (HCV) was studied to screen anti-HCV drugs (Kikuchi *et al.*, 2005). An IRES sequence from encephalomyocarditis virus (EMCV) together with the following reporter gene were ligated under the control of *rDNA* promoter to let the Pol I-mediated transcripts can translated into proteins in mammalian cells. The *rDNA* promoters from human and mouse were functioned in this system, and the human *rDNA* promoter led to an increase of neomycin phosphotransferase activity up to 70% of the Pol II-mediated protein expression system in the same plasmid (Palmer *et al.*, 1993). IRESs were also used to establish the artificial bicistronic expression system. Pol II-dependent promoter drove the two reporter genes transcription. Before the second cistron, IRES was inserted as an element for inducing the cap-independent translation initiation process in animal cells to co-express two proteins for researching bivalent drugs, vaccines and so on (Pizzato *et al.*, 1998; Guerbois *et al.*, 2013; Renaud-Gabardos *et al.*, 2015; Al-Allaf *et al.*, 2019).

Based on different secondary structures, the requirements for translation initiation factors and the manner of recruiting the ribosome, IRESs can be divided into four types. Among them, type IV IRESs, characterized by having three pseudoknots, and requiring no known translation initiation factors and initiator tRNA (Met-tRNA$_i^{Met}$), can recruit directly 40S small ribosomal subunits to the non-AUG start codon and can work in *S. cerevisiae*. The CrPV-IRES – IRES in the intergenic region (IGR) of the cricket paralysis virus (CrPV) – is a typical type IV example (Jan and Sarnow, 2002; Pestova *et al.*, 2004; Deniz *et al.*, 2009; Hertz and Thompson, 2011a,b; Thompson, 2012; Hodgman and Jewett, 2014). CrPV-IRES was also

used for establishing the artificial bicistronic expression system in *S. cerevisiae* cells to overcome the challenge of only monocistronic messages in eukaryotes. Similar as that in animal cells, a Pol II-dependent promoter (e.g. promoters of *CUP1*, *PGK1* and so on) drove the transcription of two reporter genes, and the fragment of the native CrPV-IRES was inserted just before the second one. When the second reporter gene was *URA3*, which encodes orotidine-5′-phosphate decarboxylase and allows cell growth in the absence of uracil (-Ura), the strain showed no growth phenotype on -Ura plate, until certain genes encoding cap-dependent translation initiation factors (e.g. *FUN12*-coding eIF5B; *IMT3*-, *IMT4*-coding Met-tRNA$_i^{Met}$) were deleted (Thompson *et al.*, 2001; Makelainen and Makinen, 2007; Deniz *et al.*, 2009; Mardanova *et al.*, 2009; Edwards and Wandless, 2010; Hertz and Thompson, 2011b). IRES was also tested *in vitro*: in the yeast cell-free protein synthesis system, the native CrPV-IRES allowed the translation of the reporter protein under the control of the T7 promoter with 0.92 μg ml^{-1} luciferase. Furthermore, combining the native CrPV-IRES with the just following 12 nucleotide (nt) sequence (GCTACATTTCAA) which contains the IRES-preferred initiation codon GCU, pushed luciferase translation up to 4.3 μg ml^{-1}, indicating that this 12 nt sequence was very important for the function of IRES (Martinez-Salas *et al.*, 2008; Hertz and Thompson, 2011b; Thompson, 2012; Hodgman and Jewett, 2014).

It can be imagined if there is an efficient protein expression system mediated by Pol I, the changes in regulation of rRNAs synthesis might be got indirectly but conveniently by observing the variation in a reporter gene expression. That also gives a possibility to develop a high-throughput screening model for breeding high-nucleic-acid content yeasts, when combined with flow cytometry. Therefore, in this study, the Pol I-mediated protein expression system with an IRES element was constructed in an episomal plasmid to create a monocistron of 5′ cap-independent translation initiation process in *S. cerevisiae*. The *URA3* gene was first expressed to evaluate the expression system by observing the growth phenotype in uracil deficient medium. Based on the variation of GFP fluorescence, the system was also tested for high-nucleic-acid content yeast cells in large-scale screening by flow cytometry sorting.

Results

Design statement of Pol I-mediated protein expression system

Pol I catalyses rRNA synthesis and first recognizes the transcription initiation site (TIS), therefore, the region including the TIS within a 578 nt sequence upstream of the *rDNA* gene was selected as the promoter (*rDNAp*).

The key for setting up the Pol I-mediated protein expression system is the element for translation initiation, while the internal ribosome entry site (IRES) can induce the 5′ cap-independent translation initiation. Since the 12 nt sequence (GCTACATTTCAA) containing GCU initiation codon that follow the native CrPV-IRES (192 nt) (NCBI Reference Sequence: NC_003924.1) favoured translation was confirmed *in vitro* (Hodgman and Jewett, 2014), total 204 nt fragment (named IRES12 in this study) was arranged behind *rDNAp* to induce cap-independent translation initiation. The original initiation codon ATG in the following reporter gene was therefore removed. In order to observe clearly if the Pol I-mediated expression system worked or not, the growth-based marker *URA3* was first tested. Meanwhile, the *FLAG* was also tagged at the 3′-end of *URA3* for western blot analysis. The 50 nt *oligo-dT* was artificially synthesized and introduced in the expression cassettes in order to transcribe directly into a 3′ poly-A tail for translation termination (Gan and Jewett, 2014; Hodgman and Jewett, 2014). Finally, the 284 nt fragment downstream of the *rDNA* gene was used as the terminator (Peyresaubes *et al.*, 2017). The designed Pol I-mediated *URA3* expression cassettes with intact elements are the *rDNAp*-IRES12-^{ATGΔ}*URA3* (or ^{ATGΔ}*URA3-FLAG*)-*oligo-dT-rDNAt*. The expression cassette with no IRES12, but with the original initiation codon ATG (*rDNAp- URA3- oligo-dT- rDNAt*), was used for the negative control. Meanwhile, the *URA3* under the control of the translational elongation factor EF-1 alpha promoter (*TEF1p*) transcribed by Pol II was also constructed (*TEF1p- URA3- PGK1t*) as a positive control. All the *URA3* expression cassettes were ligated into the skeleton of the yeast episomal plasmid derived from pMA91 (Mellor *et al.*, 1983) (Table 1, Line 2, 3, 4 and 5; Fig. 1).

Availability of the Pol I-mediated URA3 expression system proof by growth phenotype

The pMA91 plasmid (Fig. S1) and its derivatives (Table 1; Fig. 1) were transformed into strain BY4741 (*leu2*, *ura3*) and the recombinants were selected by the original *LEU2* selection marker. The transformants were then used for the spot dilution growth assay. All the strains grew well on the plates containing uracil (+Ura). On the plates without uracil (−Ura), as the negative and positive controls, the cells with no *URA3* showed no growth phenotype, while, the Pol II driven cassette (*TEF1p- URA3- PGK1t*) induced normal cell growth (Fig. 2A and B). The Pol I-mediated *URA3* expression cassette including the intact elements we designed also guided good cell growth, as we expected, but the strain without IRES12 exhibited no growth phenotype on the −Ura plate (Fig. 2C and D). Since disruption of some

Table 1. Plasmids and strains used in this study.

Plasmids/strains	Genotype/properties	Source/reference
Plasmids		
(1) pMA91	Episomal plasmid; *LEU2, ura3*	Mellor *et al*. (1983)
(2) pMU	pMA91 derivative; *LEU2, TEF1p-URA3-PGK1t* (Pol II mediated)	This study
(3) pMNU	pMA91 derivative; *rDNAp-URA3-oligo-dT-rDNAt* (Pol I mediated)	This study
(4) pMIU	pMA91 derivative; *LEU2, rDNAp-IRES12-*$^{ATG\Delta}$*URA3-oligo-dT-rDNAt* (Pol I mediated)	This study
(5) pMIUF	pMA91 derivative; *LEU2, rDNAp-IRES12-*$^{ATG\Delta}$*URA3- FLAG-oligo-dT-rDNAt* (Pol I mediated)	This study
(6) pMIG	pMA91 derivative; *LEU2, rDNAp-IRES12-*$^{ATG\Delta}$*yEGFP3-oligo-dT-rDNAt* (Pol I mediated)	This study
Strains		
(7) BY4741	*MATa*; *his3Δ1; leu2Δ0; met15Δ0; ura3Δ0*	EUROSCARF
(8) BXZ01	BY4741 derivative; empty plasmid {pMA91}/ (*LEU2, ura3*)	This study
(9) BXZ02	BY4741 derivative; {pMU}/ (*LEU2, URA3*$^{Pol\ II}$)	This study
(10) BXZ03	BY4741 derivative; {pMNU}/ (*LEU2, URA3*$^{ires\Delta,\ Pol\ I}$)	This study
(11) BXZ04	BY4741 derivative; {pMIU}/ (*LEU2,* $^{ATG\Delta}$*URA3*$^{IRES12,\ Pol\ I}$)	This study
(12) BXZ05	BY4741 derivative; {pMIUF}/ (*LEU2,* $^{ATG\Delta}$*URA3-FLAG*$^{IRES12,\ Pol\ I}$)	This study
(13) BXZ06	BXZ04 derivative; *imt3Δ imt4Δ::loxP-KanMX-loxP*/ (*LEU2,* $^{ATG\Delta}$*URA3*$^{IRES12,\ Pol\ I}$, *imt3Δ imt4Δ*)	This study
(14) BXZ07	BXZ04 derivative; *fun12Δ::loxP-KanMX-loxP*/ (*LEU2,* $^{ATG\Delta}$*URA3*$^{IRES12,\ Pol\ I}$, *fun12Δ*)	This study
(15) BXZ08	BY4741 derivative; {pMIG}/ (*LEU2,* $^{ATG\Delta}$*yEGFP3*$^{IRES12,\ Pol\ I}$)	This study
(16) BXZ08m1	BXZ08 derivative; after ARTP mutagenesis	This study
(17) BXZ08m2	BXZ08 derivative; after ARTP mutagenesis	This study
(18) BXZ08m3	BXZ08 derivative; after ARTP mutagenesis	This study

genes encoding cap-dependent translation initiation factors can improve IRES-mediated cap-independent translation initiation process (Thompson *et al*., 2001; Deniz *et al*., 2009), the plasmid with the intact elements for Pol I-mediated *URA3* expression cassette (*rDNAp*-IRES12-$^{ATG\Delta}$*URA3-oligo-dT-rDNAt*) (Table 1, Line 4; Fig. 1) was also introduced into the strains with eIF5B and Met-tRNA$_i^{Met}$ coding gene deletions, *fun12Δ* and *imt3Δ imt4Δ*, respectively (Table 1, Line 13, 14). The *fun12Δ* encouraged cell growth on -Ura plate more than the *imt3Δ imt4Δ* did (Fig. 2E and F) compared with the wild type (Fig. 2C). On the other hand, the strain with intact elements for Pol I-mediated *URA3-FLAG* expression cassette also showed the growth phenotype on −Ura plate (Fig. 2G), and the *URA3* coding protein (Ura3p) at its correct size (30 kDa), was directly detected from its cell lysates by western blot analysis (Fig. 2I). In contrast, the Ura3p produced by the bicistronic expression system, in which IRES guided the expression of the second cistron, can not be detected by western blot, until disruption of some genes encoding cap-dependent translation initiation factors, such as *fun12Δ* (Deniz *et al*., 2009). These results confirmed that the innovative monocistronic expression system mediated by Pol I and IRES has been successfully established in *S. cerevisiae*. Furthermore, IRES12 played a key role in the functionality of the innovative protein expression system.

Enhancement of GFP fluorescence intensity by the Pol I-mediated expression system

Based on the positive results described above, to set up a convenient large-scale screening model for high-nucleic-acid content yeast combined with flow cytometry, the reporter gene in this Pol I-mediated expression system was replaced by the GFP gene without the original initiation codon ATG ($^{ATG\Delta}$*yEGFP3*). The recombinant plasmid (Table 1, Line 6; Fig. 1A) was also transformed into the strain BY4741 and the transformants were selected by the original *LEU2* selection marker in pMA91 (Fig. S1). A total of 2×10^5 cells were monitored by the flow cytometer and the cells were analysed with Kaluza Analysis 2.1 software. Compared with the strain with empty plasmid, the resulting strain's fluorescence histogram plot drifted to higher direction (right in Fig. 3A and B). The mean fluorescence intensity (MFI) increased from 4.6 to 14.0 arbitrary units (a.u.) in average (Fig. 3B). Meanwhile, the number of cells with fluorescence intensity > 40 a.u. increased from 9 to 3540 (Fig. 3B green part, 3d). These results indicate that the GFP was also successfully expressed by the innovative Pol I-mediated system.

The cells with higher GFP expression mediated by Pol I after mutagenesis were sorted through flow cytometry and exhibited higher RNA content

Since the intracellular rRNA synthesis forms tight regulation homoeostasis by Pol I and other transcription factors, the ARTP system was used to mutagenize the strain harbouring the Pol I-mediated GFP expression cassette (*LEU2,* $^{ATG\Delta}$*yEGFP3*$^{IRES12,\ Pol\ I}$) to globally perturb the rRNA synthesis. The working dose with 90% lethality rate (Fig. S2) was used for treating the 10^4–10^5 cells by ARTP mutagenesis system. After mutagenesis, the cells were incubated in an SC liquid medium without
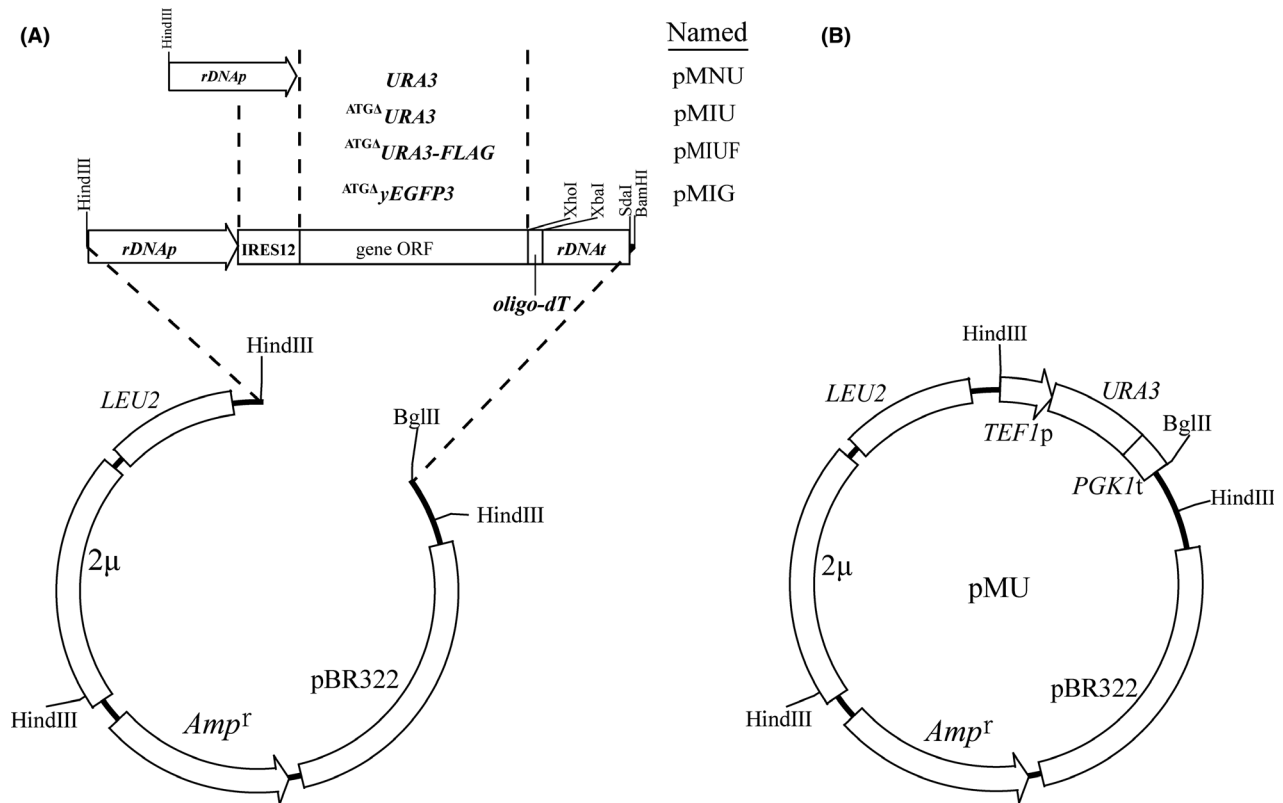
Fig. 1. The physical maps of the vectors.
A. The elements used in the Pol I-mediated protein expression cassettes: 578 nt upstream of *rDNA* gene, containing the transcription initiation site, was used as the *rDNA* promoter (*rDNAp*); the type IV IRES from CrPV (192 nt) with the just following 12 nt sequence (called **IRES12** in this study), containing GCU initiation codon (NCBI Reference Sequence: NC_003924.1) (Hodgman and Jewett, 2014), was used for inducing the 5′ cap-independent translation initiation process; the genes with no original initiation codon ATG was used as reporter genes, that is, [ATG-Δ]*URA3*, [ATGΔ]*yEGFP3* and [ATGΔ]*URA3-FLAG* with the *FLAG* tagged at the 3′-end. Meanwhile, normal **URA3**, with no IRES12, was used as negative control; 50 nt synthetic polythymine marked as ***oligo-dT***; 284 nt downstream of the *rDNA* gene was used as *rDNA* terminator (*rDNAt*).
B. The normal *URA3* expression cassette controlled by Pol II recognized *TEF1p* was used as a positive control. All the expression cassettes were ligated in the skeleton derived from the episomal plasmid pMA91 (Mellor *et al.*, 1983, Fig. S1). The genotype properties of all plasmids were also listed in Table 1.

leucine (−Leu) to recover the cell growth. The fresh cultures at mid-exponential phase were analysed by flow cytometry. The fluorescence histogram plot of 2×10^5 cells further drifted to higher direction (right in Fig. 3C), and the MFI increased from 14.0 to 22.4 a. u., which was about 1.6-fold higher than that of the strain before mutagenesis (Fig. 3C). The number of cells with fluorescence intensity > 40 a.u. reached 28,260 (Fig. 3C green and purple parts, 3D). These results indicate that mutagenesis perturbed the Pol I-mediated GFP expression even in the episomal plasmid.

Since the *rDNAp* drove the GFP expression in this monocistronic expression system, we therefore speculated that the cells with higher fluorescence intensity could also have higher RNA content. Hence the mutagenized cells with fluorescence intensity > 2000 a. u. were sorted out as high-nucleic-acid content yeast candidates. Only about 100 out of 2×10^5 cells showed such a

feature and were dropped separately onto the plates. Among several dozens of the grown colonies, 12 colonies were randomly selected to detect the MFI, and three (BXZ08m1-3) of them, especially BXZ08m3, showed higher MFI than the parental strain BXZ08 ([ATG-Δ]*yEGFP3*[IRES12, Pol I]) (Fig. 4A, black columns). Not unexpectedly, their total RNA content had increased significantly, especially that of BXZ08m3 reached 176.8 mg g^{-1} DCW, with a 58% improvement compared to the BXZ08 (Fig. 4B, black columns). Meanwhile, three mutants showed almost the same MFI and total RNA content before and after 10 days of subculture (Fig. 4). The sequence variation of all elements in the expression cassette, especially *rDNAp* and IRES12, could be one of the reasons for the enhanced GFP expression level. However, the DNA sequencing results showed no changes in the Pol I-mediated *yEGFP3* expression cassettes in plasmids rescued from the mutants BXZ08m1-3
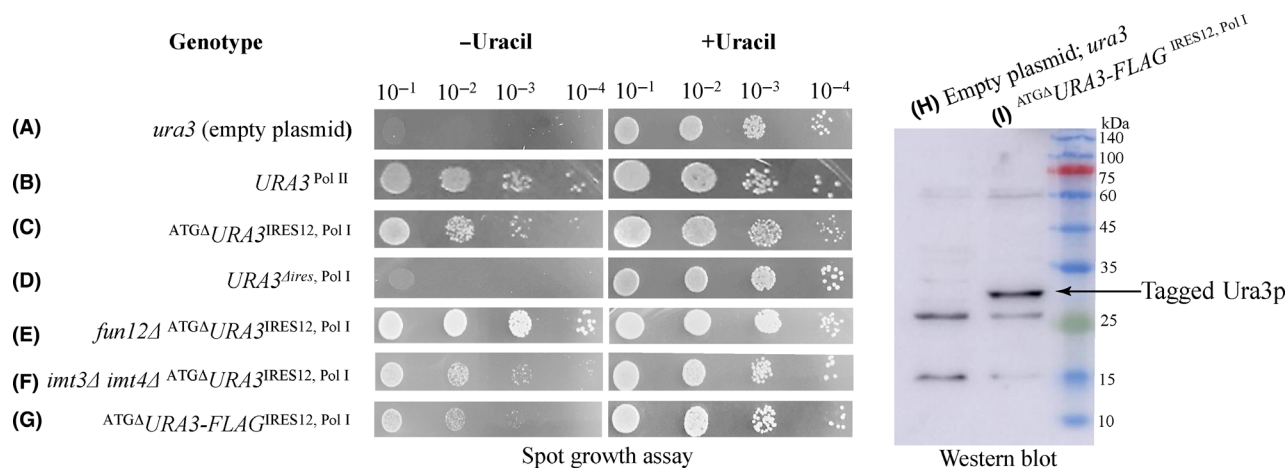
Genotype	−Uracil				+Uracil			
	10^{-1}	10^{-2}	10^{-3}	10^{-4}	10^{-1}	10^{-2}	10^{-3}	10^{-4}
(A) *ura3* (empty plasmid)								
(B) *URA3*^{Pol II}								
(C) ^{ATGΔ}*URA3*^{IRES12, Pol I}								
(D) *URA3*^{Δires, Pol I}								
(E) *fun12Δ* ^{ATGΔ}*URA3*^{IRES12, Pol I}								
(F) *imt3Δ imt4Δ* ^{ATGΔ}*URA3*^{IRES12, Pol I}								
(G) ^{ATGΔ}*URA3-FLAG*^{IRES12, Pol I}								

Spot growth assay   Western blot

Fig. 2. The Pol I-mediated *URA3* expression system worked well. The spot growth assay on SC medium supplemented without (*left*) or with (*right*) uracil. The cells were serially 10-fold diluted from an initial OD$_{600}$ 1.0, then spotted on the plates and incubated for 2 days at 30°C. The cell lysates were detected by western blot analysis.
A and H. cells with empty plasmid, thus devoid of *URA3*.
B. cells harbouring plasmid with Pol II-mediated *URA3* expression cassette.
C. cells harbouring plasmid (i.e. pMIU in Table 1, Line 4) with intact elements for Pol I-mediated expression cassette.
D. cells harbouring plasmid with the Pol I-mediated cassette but no IRES12.
E. cells with pMIU lacking eIF5B (*fun12Δ*).
F. cells with pMIU lacking Met-tRNA$_i$^Met (*imt3Δ imt4Δ*).
G and I. cells harbouring pMIUF (in Table 1, Line 5) that the *FLAG* was tagged at the 3′-end of *URA3* in pMIU also showed growth phenotype and the correct size of the Ura3p in its cell lysate detected by western blot analysis.

and their parental strain BXZ08 (Fig. S3). These results indicate that mutagenesis could probably induce some changes in other factors and thus alter rRNA synthesis regulation homoeostasis. Coupling the innovative Pol I and IRES-mediated monocistronic GFP expression system with flow cytometry, a large-scale screening model for *S. cerevisiae* with high-nucleic-acid content worked well.

Discussion

IRESs are the 5′ cap-independent translation initiation elements. In particular, the native CrPV-IRES, found in the IGR of CrPV, led the translation of the second reporter gene in the Pol II-mediated dicistronic expression system in *S. cerevisiae*. However, its emerging validity should cooperate with the disruption of some cap-dependent translation initiation factors (Thompson *et al.*, 2001; Deniz *et al.*, 2009). A more effective element called IRES12 (the native CrPV-IRES with the just following 12 nt sequence) already tested *in vitro* in yeast cell-free protein synthesis system (Hodgman and Jewett, 2014), was used for inducing the translation in the IRES and Pol I-mediated monocistronic expression system in this study. Normally, Pol I can only transcribe rRNA, but by using the IRES and Pol I-mediated monocistronic expression system, we showed that proteins could be smoothly synthesized (Fig. 2I), and we highlighted the unnecessary disruption of some cap-

dependent translation initiation factors (Fig. 2C). Nevertheless, deletion of eIF5B (*fun12Δ*) indeed enhanced cell growth phenotypes (Fig. 2E), indicating that the cap-dependent translation initiation factors also have a negative impact on such cap-independent translation induced by IRES12, the more effective IRES element. In fact, it was demonstrated that, in the dicistronic expression system, the efficiency reduction of cap-dependent initiation can also enhance the activity of CrPV-IRES, even if it does not require any known translation initiation factors. Cap-dependent and cap-independent translation initiation competed with each other due to the limited number of unemployed ribosomes *in vivo* (Thompson *et al.*, 2001; Jan and Sarnow, 2002; Deniz *et al.*, 2009). On the other hand, it was reported that IRES-mediated cap-independent translation initiation in eukaryotes generally functions when cells encounter some stress such as heat shock, hypoxia and nutrient deprivation (Holcik *et al.*, 1999; Holcik and Sonenberg, 2005; Gilbert *et al.*, 2007; Reineke *et al.*, 2011). We suggest that if the stress-related gene is used as a selective marker, the expression system might work better under stress conditions.

By combining the innovative IRES and Pol I-mediated monocistronic expression system with flow cytometry, a large-scale screening model for high-nucleic-acid content yeasts based on the change of GFP green fluorescence intensity has been successfully established. After ARTP mutagenesis, about 100 yeast cells with fluorescence
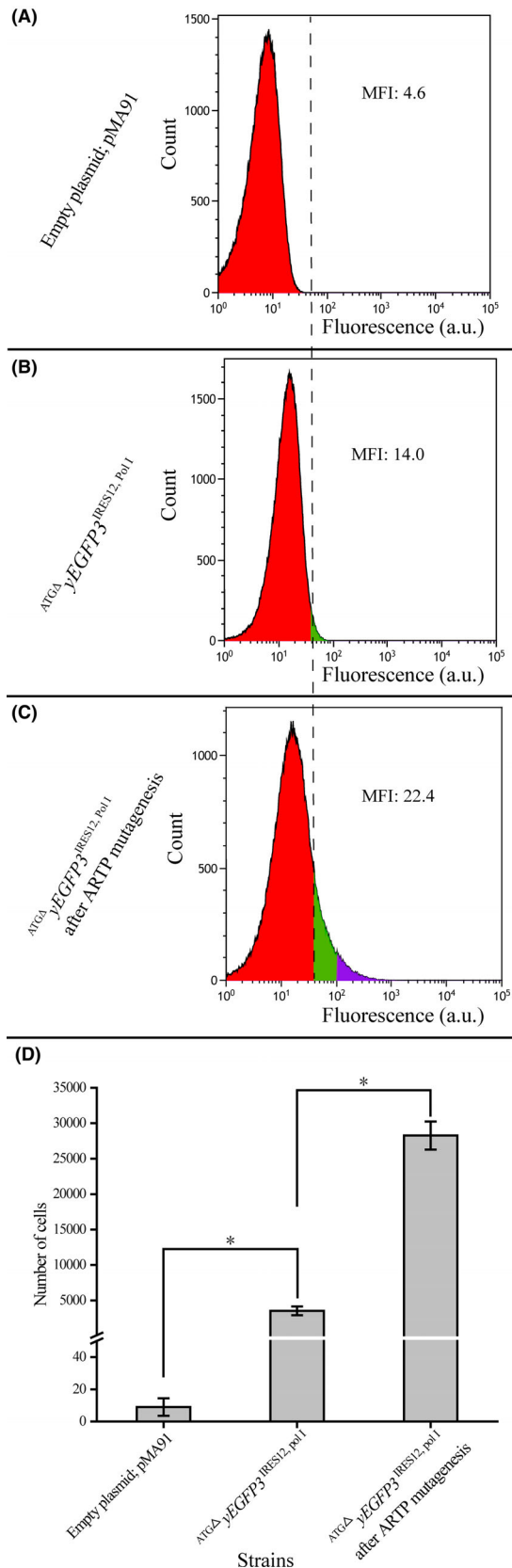
Fig. 3. Flow cytometry analysis of the Pol I-mediated GFP expression system. The fluorescence histogram plot of the cells with (A) empty plasmid, (B) plasmid harbouring Pol I-mediated GFP expression cassette, and (C) after mutagenesis. The dashed line marks the fluorescence intensity of 40 arbitrary units (a.u.). The cells with fluorescence intensity > 40 a.u. are represented in green, while those with fluorescence intensity > 100 a.u. are represented in purple. MFI: mean fluorescence intensity. (D) The number of cells with fluorescence intensity > 40 a.u. The data from the five independent cultivations were compared using the Mann–Whitney U test. *$P < 0.05$ was considered statistically significant. A total of 2×10^5 cells were analysed by the flow cytometer with Kaluza Analysis 2.1 software.

intensity > 2000 a. u. caught our attention; among them, the BXZ08m3 strain with 176.8 mg g^{-1} DCW total RNA content was selected through simple fluorescence intensity test and RNA content measurement, which was with 58% improvement compared to the parental strain BXZ08. Meanwhile, the data kept steady at least after 10 days of subculture (Fig. 4). Importantly, since there are strong or weak promoters in single-nucleotide polymorphism, the *rDNAp* sequence controlling the *yEGFP3* in these high-nucleic-acid content yeast episomal plasmids did not change (Fig. S3). Besides, the sequences of other introduced elements also showed no variation. These results indicated that mutagenesis might perturb the rRNA biosynthesis homoeostasis.

Conclusions

In this study, an innovative IRES and Pol I-mediated monocistronic expression system for large-scale screening of high-nucleic-acid content yeasts has been designed and established, in which the elements included *rDNAp*, IRES12 from CrPV carrying its preferred initiation codon GCU, reporter genes without their original initiation codon ATG, *oligo-dT* and *rDNAt*. The regulatory changes of rRNA synthesis perturbed by mutagenesis were monitored by observing the variation in the expression status of GFP. In combination with flow cytometry, the BXZ08m3 strain which showed a 58% improvement in total RNA content has been efficiently sorted out and exhibited no sequence alteration in the Pol I-mediated *yEGFP3* expression cassette in the episomal plasmid. This provides at least two meaningful enlightenment. First, the episomal plasmid containing *yEGFP3* (Table 1, Line 6) can be easily lost under non-selective pressure condition continuously (Dani and Zakian, 1983) to get a non-transgenic high-nucleic acid industrial strain (wild type, polyploidy), which might be very beneficial in food industry for health so far. Second, these high-nucleic-acid content yeasts could be the useful research materials in the study of the rRNA synthesis regulation mechanism, as in omics analysis.
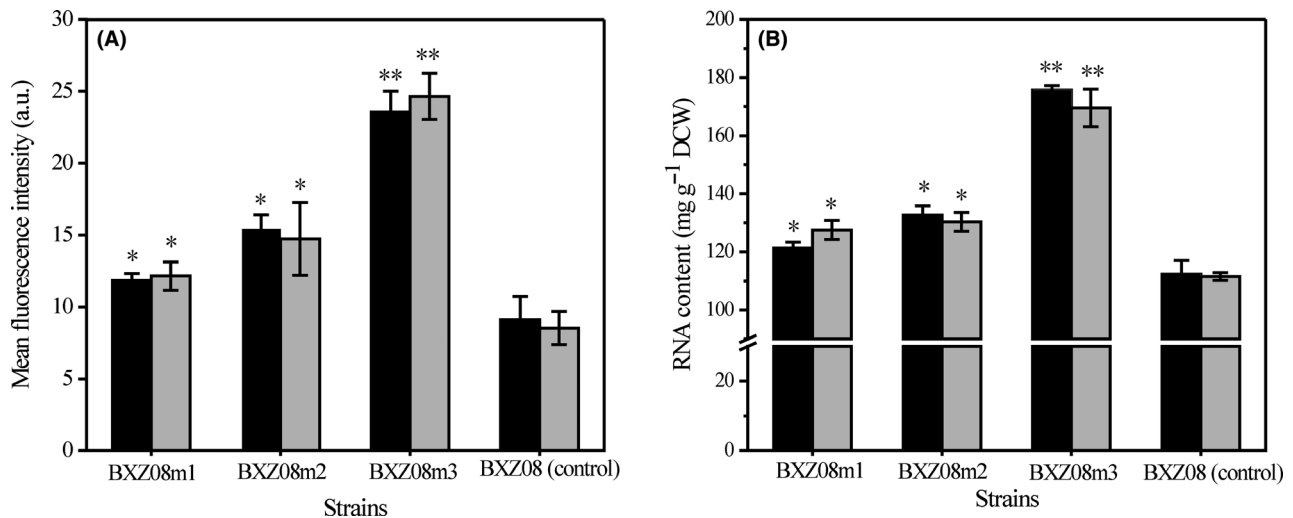
Fig. 4. The cells with higher mean fluorescence intensity (A) also exhibited higher total RNA content (B). The mutants BXZ08m1-3 were single cells with higher fluorescence intensity sorted from the parental strain BXZ08 ($^{ATG\Delta}yEGFP3^{IRES12, Pol I}$) after mutagenesis. The black columns stand for the first generation cells and the grey columns stand for the cells continuously transferred to fresh medium after 10 days. The coefficients of the 1.0 OD_{600} to dry cell weight (DCW) were $\pm 1.38 \times 10^{-4}$ g for all the tested strains. The data from the independent triplicate cultivations were compared using one-way ANOVA followed by LSD post hoc test. *$P < 0.05$ was considered statistically significant. **$P < 0.01$ was considered highly significant.

Experimental procedures

Plasmid/strain construction and media

In this study, the skeleton of the yeast episomal plasmid was pMA91 with a *LEU2* marker (Mellor *et al.*, 1983), but without the *PGK1* promoter (*PGK1p*), which was removed by partial digestion with BglII and HindIII (Fig. S1). The fragments of *URA3* and *yEGFP3* without the original initiation codon ATG ($^{ATG\Delta}URA3$ and $^{ATG\Delta}yEGFP3$) were respectively amplified from plasmids pJFE3 (Shen *et al.*, 2012) and pJFE3-*yEGFP3* (Wang *et al.*, 2013). The different Pol I-mediated gene expression cassettes (Fig. 1A) were ligated to the skeleton between the BglII and HindIII sites in three steps. (i) First, the fragments containing *rDNAp*, IRES12, reporter genes ($^{ATG\Delta}URA3$ and $^{ATG\Delta}yEGFP3$), but devoid of *oligo-dT* and *rDNAt* were obtained by overlap extension polymerase chain reaction (OE-PCR), in which XhoI, SdaI and BamHI restriction sites were respectively introduced to the 3'-end of the reporter genes, and ligated to the skeleton between the BglII and HindIII sites (Fig. S1). (ii) Subsequently, to reduce undesired mutations occurred in *oligo-dT*, the sequence was artificially synthesized and constructed in pUC19, and the *rDNAt* fragment was amplified and ligated to the *oligo-dT* containing plasmid between XbaI and SdaI sites. (iii) Finally, the XhoI/SdaI-digested fragment of *oligo-dT-rDNAt* was inserted between XhoI and SdaI sites which located downstream of the reporter genes, resulting in the individual completed expression plasmids (Fig. 1A).

Meanwhile, a normal *URA3* expression cassette controlled by Pol II recognized *TEF1p* (Translational Elongation Factor 1-alpha promoter) was also ligated between the BglII and HindIII sites (Fig. 1B). The plasmids constructed in this study are listed in Table 1, and the primers used in this study are listed in Table S1.

The *S. cerevisiae* strain BY4741 (*MATa*, *his3Δ1*; *leu2Δ0*; *met15Δ0*; *ura3Δ0*) (EUROSCARF, Frankfurt am Main, Germany) was used as the host. Following methods described in our previous work (Peng *et al.*, 2012), the three disruption cassettes FUN12F-*loxP-KanMX-loxP*-FUN12R, IMT3F-*loxP-KanMX-loxP*-IMT3R and IMT4F-*loxP-KanMX-loxP*-IMT4R were obtained from PCR by using the three pairs of primers containing the upstream and downstream sequences of the relevant genes as recombinant arms. The disruption cassettes were then transformed into BY4741 by the dominant selection marker *KanMX* (Güldener *et al.*, 1996) to disrupt the genes *FUN12* (encoding the translation initiation factor eIF5B) and *IMT3/IMT4* (encoding the Met-tRNA$_i^{Met}$) (Thompson *et al.*, 2001; Deniz *et al.*, 2009). The empty and recombinant plasmids were transformed into BY4741 and its derivatives, the *fun12Δ* and *imt3Δ/4Δ* deletion strains, and were selected by the original *LEU2* selection marker in pMA91. All *S. cerevisiae* strains used in this study are listed in Table 1, and the primers used in this study are listed in Table S1.

Yeast extract peptone dextrose (YPD) (20 g l^{-1} glucose, 10 g l^{-1} yeast extract, 20 g l^{-1} peptone) and synthetic complete (SC) (20 g l^{-1} glucose, 1.7 g l^{-1} yeast

nitrogen base, 5 g l^{-1} ammonium sulfate, supplemented respectively 0.77 g l^{-1} CSM-Ura or CSM-Leu (Sunrise Science Products, USA) media were used to cultivate the yeast cells.

Spot dilution growth assay

The overnight cultures were inoculated in fresh liquid medium and cultured to the mid-exponential phase (OD_{600} 0.8–1.0), centrifuged, washed and resuspended in 1.0 ml sterile water for 9 h to consume the intracellular nutrients. The cell density was normalized to OD_{600} 1.0. The 4 μl of serial 10-fold dilutions were spotted onto the appropriate plates and incubated at 30 °C.

Cell disruption and western blot analysis

Cells were cultured to the mid-exponential phase, then disrupted by vortexing with glass beads in a 4°C cold breaking buffer (20 mmol l^{-1} Tris-HCl, pH 7.9, 10 mmol l^{-1} MgCl$_2$, 1 mmol l^{-1} EDTA, 1 mmol l^{-1} PMSF, 1 mmol l^{-1} DTT, 0.3 mmol l^{-1} (NH$_4$)$_2$SO$_4$, 5% glycerol phosphate). In total, the cell lysates containing 100 μg proteins were analysed by SDS-PAGE and transferred to a polyvinylidene fluoride membrane, using an anti-FLAG antibody at 1:2500 dilution, antibody IgG (H + L) HRP at 1:10,000 dilution (both from ABclonal Biotechnology, China), and finally detected with the Amersham Imager 600 imaging system (GE Healthcare, USA) (MacPhee, 2010).

Cell fluorescence intensity analysis and cell sorting via flow cytometry

Cells were cultured in SC medium minus leucine (−Leu) and harvested at mid-exponential phase, washed twice with ice-cold 10 mmol l^{-1} phosphate buffer (PBS, pH 7.0) and resuspended in PBS. Samples of 2×10^5 cells were monitored through the FITC (Fluorescein isothiocyanate) channel (excitation and emission wavelengths of GFP were 488 and 507 nm, respectively) (Zhang *et al.*, 2015) via flow cytometer (MoFlo™ XDP High-Performance Cell Sorter, Beckman Coulter, USA) and analysed with the Kaluza Analysis 2.1 software. The mean fluorescence intensity (MFI) was the sum of fluorescence intensity for each single cell divided by the 2×10^5 analysed cells. Meanwhile, the cells with fluorescence intensity > 2000 a.u. were sorted out as high-nucleic-acid content yeast candidates.

ARTP mutagenesis process

ARTP (ARTP-IIS Wuxi Tmaxtree Biotechnology, Wuxi, China) is an effective and now widely used physical mutagenic system (Zhang *et al.*, 2014; Guo *et al.*, 2019). The 10 SLM (standard litre per minute) high-purity helium as the plasma working gas, 90W of the radio frequency power input, and 3.5 mm distance between the plasma torch nozzle and the treated sample plates were used in this study. Briefly, cells were cultured to mid-exponential phase and harvested. About 10^4–10^5 cells suspended in 5% glycerol were spread on a sterilized sample plate and treated with the ARTP system. The lethality rate was calculated as untreated colonies (total cells) minus treated colonies (survived cells), divided by the total cells which were grown on YPD plates (Chen *et al.*, 2010). An exposure time of 20 s with 90% lethality rate (Fig. S2) was used as the working dose. After treatment, the samples were washed with 1 ml sterile water and inoculated into a SC liquid medium minus leucine (−Leu), then incubated for 2 days at 30°C, after which the cells were transferred to the medium again, the fresh culture in mid-exponential phase were ready for flow cytometry analysis.

Meanwhile, the high-nucleic-acid content mutants were continuously subcultured. Once the cells reached the stationary phase, a new batch was started by transferring the culture into fresh medium. After 10 days, the fresh cultures in mid-exponential phase were also harvested for the MFI test and total RNA content measurement.

Extraction and measurement of total RNAs

Total intracellular RNAs were extracted with perchloric acid (PCA) (Herbert *et al.*, 1971; Chuwattanakul *et al.*, 2011). Briefly, 1.0 OD_{600} cells were suspended in 1 ml of 0.25 mol l^{-1} ice-cold PCA for 30 min and centrifuged. The cell pellets were then resuspended in 1.0 ml of 0.5 mol l^{-1} PCA at 70°C for 20 min. After centrifugation at 12,000 r.p.m. for 2 min, the absorbance at 260 nm of the supernatant, multiplied by a 0.04 coefficient (Eppendorf BioPhotometer D30), was the determined RNA content (mg) of 1.0 OD_{600} cells. The dry cell weight (DCW) of strains were determined according to a previously reported method (Xu *et al.*, 2014). The RNA content value was then divided by the DCW to get the RNA content (mg g^{-1} DCW).

Statistical analysis

Statistical significance was determined by Mann–Whitney *U* test for the differences between two groups and by one-way ANOVA and post hoc LSD test (homogeneity of variance) for differences between multiple groups using the software SPSS (SPSS Inc, Chicago, USA). Error bars denote mean ± standard deviation. $P < 0.05$ was considered statistically significant (*$P < 0.05$; **$P < 0.01$).

Acknowledgements

Conflict of interest

None declared.

References

Aitken, C.E., and Lorsch, J.R. (2012) A mechanistic overview of translation initiation in eukaryotes. *Nat Struct Mol Biol* **19:** 568.

Akiyama, S., Doi, M., Arai, Y., Nakao, Y., and Fukuda, H. (1975) Production of yeast biomass. Google Patents.

Al-Allaf, F.A., Abduljaleel, Z., Athar, M., Taher, M.M., Khan, W., Mehmet, H., *et al.* (2019) Modifying inter-cistronic sequence significantly enhances IRES dependent second gene expression in bicistronic vector: Construction of optimised cassette for gene therapy of familial hypercholesterolemia. *Noncoding RNA Res* **4:** 1–14.

Buratowski, S. (2009) Progression through the RNA polymerase II CTD cycle. *Mol Cell* **36:** 541–546.

Cairoli, P., Pieraccini, S., Sironi, M., Morelli, C.F., Speranza, G., and Manitto, P. (2008) Studies on umami taste. Synthesis of new guanosine 5′-phosphate derivatives and their synergistic effect with monosodium glutamate. *J Agric Food Chem* **56:** 1043–1050.

Chen, H., Bai, F., and Xiu, Z. (2010) Oxidative stress induced in *Saccharomyces cerevisiae* exposed to dielectric barrier discharge plasma in air at atmospheric pressure. *ITPS* **38:** 1885–1891.

Chuwattanakul, V., Kim, Y.-H., Sugiyama, M., Nishiuchi, H., Miwa, H., Kaneko, Y., and Harashima, S. (2011) Construction of a *Saccharomyces cerevisiae* strain with a high level of RNA. *J Biosci Bioeng* **112:** 1–7.

Dani, G.M., and Zakian, V.A. (1983) Mitotic and meiotic stability of linear plasmids in yeast. *Proc Natl Acad Sci USA* **80:** 3406–3410.

Deniz, N., Lenarcic, E.M., Landry, D.M., and Thompson, S.R. (2009) Translation initiation factors are not required for Dicistroviridae IRES function *in vivo*. *RNA* **15:** 932–946.

Edwards, S.R., and Wandless, T.J. (2010) Dicistronic regulation of fluorescent proteins in the budding yeast *Saccharomyces cerevisiae*. *Yeast* **27:** 229–236.

Gan, R., and Jewett, M.C. (2014) A combined cell-free transcription-translation system from *Saccharomyces cerevisiae* for rapid and robust protein synthe. *Biotechnol J* **9:** 641–651.

Gilbert, W.V., Zhou, K., Butler, T.K., and Doudna, J.A. (2007) Cap-independent translation is required for starvation-induced differentiation in yeast. *Science* **317:** 1224–1227.

Guerbois, M., Volkova, E., Forrester, N.L., Rossi, S.L., Frolov, I., and Weaver, S.C. (2013) IRES-driven expression of the capsid protein of the Venezuelan equine encephalitis virus TC-83 vaccine strain increases its attenuation and safety. *PLoS Negl Trop Dis* **7:** e2197.

Güldener, U., Heck, S., Fielder, T., Beinhauer, J., and Hegemann, J.H. (1996) A new efficient gene disruption cassette for repeated use in budding yeast. *Nucleic Acids Res* **24:** 2519–2524.

Guo, J., Luo, W., Wu, X.M., Fan, J., Zhang, W.X., and Suyama, T. (2019) Improving RNA content of salt-tolerant *Zygosaccharomyces rouxii* by atmospheric and room temperature plasma (ARTP) mutagenesis and its application in soy sauce brewing. *World J Microbiol Biotechnol* **35:** 180.

Hannan, K.M., Hannan, R.D., and Rothblum, L.I. (1998) Transcription by RNA polymerase I. *Front Biosci* **3:** d376–d398.

Heidemann, M., Hintermair, C., Voss, K., and Eick, D. (2013) Dynamic phosphorylation patterns of RNA polymerase II CTD during transcription. *Biochim Biophys Acta* **1829:** 55–62.

Herbert, D., Phipps, P., and Strange, R. (1971) Chapter III chemical analysis of microbial cells. In *Methods in Microbiology*. **5** Part B, Elsevier, pp. 209–344.

Hertz, M.I., and Thompson, S.R. (2011a) Mechanism of translation initiation by Dicistroviridae IGR IRESs. *Virology* **411:** 355–361.

Hertz, M.I., and Thompson, S.R. (2011b) *In vivo* functional analysis of the Dicistroviridae intergenic region internal ribosome entry sites. *Nucleic Acids Res* **39:** 7276–7288.

Hodgman, C.E., and Jewett, M.C. (2014) Characterizing IGR IRES-mediated translation initiation for use in yeast cell-free protein synthesis. *New Biotechnol* **31:** 499–505.

Holcik, M., and Sonenberg, N. (2005) Translational control in stress and apoptosis. *Nat Rev Mol Cell Biol* **6:** 318–327.

Holcik, M., Lefebvre, C., Yeh, C., Chow, T., and Korneluk, R.G. (1999) A new internal-ribosome-entry-site motif potentiates XIAP-mediated cytoprotection. *Nat Cell Biol* **1:** 190–192.

Jan, E., and Sarnow, P. (2002) Factorless ribosome assembly on the internal ribosome entry site of cricket paralysis virus. *J Mol Biol* **324:** 889–902.

Khatun, F., Kurata, K., Chuwattanakul, V., Sugiyama, M., Kaneko, Y., and Harashima, S. (2013) Increased transcription of *RPL40A* and *RPL40B* is important for the improvement of RNA production in *Saccharomyces cerevisiae*. *J Biosci Bioeng* **116:** 423–432.

Kikuchi, K., Umehara, T., Fukuda, K., Kuno, A., Hasegawa, T., and Nishikawa, S. (2005) A hepatitis C virus (HCV) internal ribosome entry site (IRES) domain III-IV-targeted aptamer inhibits translation by binding to an apical loop of domain IIId. *Nucleic Acids Res* **33:** 683–692.

Li, B., Chen, X., Ren, H., Li, L., Xiong, J., Bai, J., *et al.* (2012) Kinetic models of ribonucleic acid fermentation

and continuous culture by *Candida tropicalis* no. 121. *Bioprocess Biosystems Eng* **35:** 415–422.

Li, B., Liu, Y., Wang, L., Hong, J., Chen, Y., and Ying, H. (2019) RNA accumulation in *Candida tropicalis* based on cofactor engineering. *FEMS Yeast Res* **19:** foz028.

MacPhee, D.J. (2010) Methodological considerations for improving Western blot analysis. *J Pharmacol Toxicol Methods* **61:** 171–177.

Makelainen, K.J., and Makinen, K. (2007) Testing of internal translation initiation via dicistronic constructs in yeast is complicated by production of extraneous transcripts. *Gene* **391:** 275–284.

Mardanova, E.S., Zamchuk, L.A., and Ravin, N.V. (2009) The leader sequence of maize alcohol dehydrogenase gene ensures internal initiation of mRNA translation in yeast cells. *Dokl Biochem Biophys* **426:** 161–163.

Martinez-Salas, E., Pacheco, A., Serrano, P., and Fernandez, N. (2008) New insights into internal ribosome entry site elements relevant for viral gene expression. *J Gen Virol* **89:** 611–626.

Mellor, J., Dobson, M., Roberts, N., Tuite, M., Emtage, J., White, S., *et al.* (1983) Efficient synthesis of enzymatically active calf chymosin in *Saccharomyces cerevisiae*. *Gene* **24:** 1–14.

Nagodawithana, T. (1992) Yeast-derived flavors and flavor enhancers and their probable mode of action. *Food Technol* **46:** 138–144.

Ohlmann, T. (2000) An internal ribosome entry segment promotes translation of the Simian Immunodeficiency Virus Genomic RNA. *J Biol Chem* **275:** 11899–11906.

Olmedo, F., Iturbe, F., Gomez-Hernandez, J., and Lopez-Munguia, A. (1994) Continuous production of 5'-ribonucleotides from yeast RNA by hydrolysis with immobilized 5'-phosphodiesterase and 5'-adenylate deaminase. *World J Microbiol Biotechnol* **10:** 36–40.

Palmer, T.D., Miller, A.D., Reeder, R.H., and McStay, B. (1993) Efficient expression of a protein coding gene under the control of an RNA polymerase I promoter. *Nucleic Acids Res* **21:** 3451–3457.

Pelletier, J., and Sonenberg, N. (1988) Internal initiation of translation of eukaryotic mRNA directed by a sequence derived from poliovirus RNA. *Nature* **334:** 320–325.

Peng, B., Shen, Y., Li, X., Chen, X., Hou, J., and Bao, X. (2012) Improvement of xylose fermentation in respiratory-deficient xylose-fermenting *Saccharomyces cerevisiae*. *Metab Eng* **14:** 9–18.

Pestova, T.V., Lomakin, I.B., and Hellen, C.U. (2004) Position of the CrPV IRES on the 40S subunit and factor dependence of IRES/80S ribosome assembly. *EMBO Rep* **5:** 906–913.

Petes, T.D. (1979) Yeast ribosomal DNA genes are located on chromosome XII. *Proc Natl Acad Sci USA* **76:** 410–414.

Peyresaubes, F., Zeledon, C., Guintini, L., Charton, R., Muguet, A., and Conconi, A. (2017) RNA Polymerase-I-dependent transcription-coupled nucleotide excision repair of UV-Induced DNA lesions at transcription termination sites, in *Saccharomyces cerevisiae*. *Photochem Photobiol* **93:** 363–374.

Pfingsten, J.S., Costantino, D.A., and Kieft, J.S. (2006) Structural basis for ribosome recruitment and manipulation by a viral IRES RNA. *Science* **314:** 1450–1454.

Pizzato, M., Franchin, E., Calvi, P., Boschetto, R., Colombo, M., Ferrini, S., and Palu, G. (1998) Production and characterization of a bicistronic Moloney-based retroviral vector expressing human interleukin 2 and herpes simplex virus thymidine kinase for gene therapy of cancer. *Gene Ther* **5:** 1003–1007.

Planta, R.J. (1997) Regulation of ribosome synthesis in yeast. *Yeast* **13:** 1505–1518.

Reineke, L.C., Cao, Y., Baus, D., Hossain, N.M., and Merrick, W.C. (2011) Insights into the role of yeast eIF2A in IRES-mediated translation. *PLoS One* **6:** e24492.

Renaud-Gabardos, E., Hantelys, F., Morfoisse, F., Chaufour, X., Garmy-Susini, B., and Prats, A.C. (2015) Internal ribosome entry site-based vectors for combined gene therapy. *World J Exp Med* **5:** 11–20.

Reynolds, J.E., Kaminski, A., Kettinen, H.J., Grace, K., Clarke, B.E., Carroll, A.R., *et al.* (1995) Unique features of internal initiation of hepatitis C virus RNA translation. *EMBO J* **14:** 6010–6020.

Rudolph, F.B., Kulkarni, A.D., Fanslow, W.C., Pizzini, R.P., Kumar, S., and Van Buren, C.T. (1990) Role of RNA as a dietary source of pyrimidines and purines in immune function. *Nutrition (Burbank)* **6:** 45–52; discussion 59–62.

Shen, Y., Chen, X., Peng, B., Chen, L., Hou, J., and Bao, X. (2012) An efficient xylose-fermenting recombinant *Saccharomyces cerevisiae* strain obtained through adaptive evolution and its global transcription profile. *Appl Microbiol Biotechnol* **96:** 1079–1091.

Sims, R.J. 3rd, Mandal, S.S., and Reinberg, D. (2004) Recent highlights of RNA-polymerase-II-mediated transcription, *Curr Opin Cell Biol* **16**: 263–271.Thompson, S.R., (2012) Tricks an IRES uses to enslave ribosomes. *Trends Microbiol* **20:** 558–566.

Thompson, S.R. (2012) Tricks an IRES uses to enslave ribosomes. *Trends Microbiol* **20:** 558–566.

Thompson, S.R., Gulyas, K.D., and Sarnow, P. (2001) Internal initiation in *Saccharomyces cerevisiae* mediated by an initiator tRNA/eIF2-independent internal ribosome entry site element. *Proc Natl Acad Sci USA* **98:** 12972–12977.

Wang, C., Shen, Y., Hou, J., Suo, F., and Bao, X. (2013) An assay for functional xylose transporters in *Saccharomyces cerevisiae*. *Anal Biochem* **442:** 241–248.

Warner, J.R. (1999) The economics of ribosome biosynthesis in yeast. *Trends Biochem Sci* **24:** 437–440.

Xu, L., Shen, Y., Hou, J., Peng, B., Tang, H., and Bao, X. (2014) Secretory pathway engineering enhances secretion of cellobiohydrolase I from *Trichoderma reesei* in *Saccharomyces cerevisiae*. *J Biosci Bioeng* **117:** 45–52.

Zhang, X., Zhang, X.F., Li, H.P., Wang, L.Y., Zhang, C., Xing, X.H., and Bao, C.Y. (2014) Atmospheric and room temperature plasma (ARTP) as a new powerful mutagenesis tool. *Appl Microbiol Biotechnol* **98:** 5387–5396.

Zhang, G., Lin, Y., Qi, X., Wang, L., He, P., Wang, Q., and Ma, Y. (2015) Genome shuffling of the nonconventional yeast *Pichia anomala* for improved sugar alcohol production. *Microb Cell Fact* **14:** 112.

Zhao, J., and Fleet, G.H. (2005) Degradation of RNA during the autolysis of *Saccharomyces cerevisiae* produces predominantly ribonucleotides. *J Ind Microbiol Biotechnol* **32:** 415–423.

Supporting information

Additional supporting information may be found online in the Supporting Information section at the end of the article.

Fig. S1. The skeleton of the yeast episomal plasmid in this study. Physical maps of plasmid (a) pMA91 (Mellor *et al.*, 1983), and (b) the skeleton derived from pMA91 with no *PGK1* promoter.

Fig. S2. The lethality curve of the ARTP treatment. The ARTP-IIS Wuxi Tmaxtree Biotechnology, Wuxi, China mutagenesis system was used to deal with 10^4-10^5 cells harbouring the Pol I-mediated GFP expression cassette (Table 1, Line 15), with the distance of 3.5 mm between plasma nozzle and the sample plates.

Fig. S3. The 1850 bp DNA sequences from promoter to terminator in the Pol I-mediated *yEGFP3* expression system in mutants BXZ08m1-3 did not generate any changes after mutagenesis, compared with their parental strain BXZ08 ($^{ATG\Delta}yEGFP3^{IRES12, Pol I}$).

Table S1. List of primers used in this study.